International Journal of Energy and Environmental Engineering
https://doi.org/10.1007/s40095-022-00499-0

ORIGINAL RESEARCH

Optimisation of wasted air utilisation in thermal loss reduction in double-glazed windows of commercial buildings in cold regions

Mohammed Lami[1] · Faris Al-naemi[1] · Hussein A. Jabbar[2] · Hameed Alrashidi[3] · Walid Issa[1]

Received: 1 March 2022 / Accepted: 15 April 2022

Abstract

Ventilating of multi pane-glazed windows using wasted air of buildings is an effective technique to minimize heat loss through windows and save heating energy in cold regions. In low-scaled occupancy buildings with high WWR ratio, buildings supply a low flow rate of wasted air to windows ventilation systems, resulting in a declination in its thermal performance. Therefore, this study introduces methods of managing the utilisation of wasted air in windows ventilation to optimise the energy saving. Two methods have been implemented experimentally on a small-scaled room. The first method is a time-based division of air pump operation, an air pump ventilates multiple windows, one window at a time repetitively. The second method shares the available wasted air to multiple windows. The experimental results and mathematical heat transfer model have been employed to evaluate thermal performance of the system in different methods. The first method showed a best energy saving with a duty cycle of 50% for the air pump, and on/off operation every 10 s. An energy saving of 42.6% has been realized compared to the traditional double-glazed windows, and the heat transfer coefficient was declined from 3.82 to 2.8 W/m^2 K. The second method showed an optimum thermal performance when the available flow rate of wasted air was shared with three double-glazed windows. An energy saving of 83.1% was achieved compared to the traditional double-glazed windows, and the heat transfer coefficient dropped from 3.82 to 2.36 W/m^2 K.

Keywords Wasted air · Forced ventilation · Ventilated double-glazed windows · Energy saving

Introduction

With the increase in energy consumption in buildings, numerous studies have been focused recently on energy saving in buildings. In modern cities, the energy consumption of buildings becomes higher than transportation and industry sections. In China, the energy demand of buildings is 28.6% of the total energy consumption [1]. In addition, the International Energy Agency (IEA) stated that the buildings that are used for accommodation purposes required 20% of the overall energy consumption in Japan, China, Russia, India, and the USA [2]. In 2013, a study revealed that 40% of energy consumption in Taiwan goes to commercial and residential buildings [3]. The energy department in the USA stated that the energy consumption of buildings in industrial countries can reach 40% [4, 5].

The energy consumption of a building is influenced by different parameters. A study shows the impact of opting of the glazing type on the power consumption of a modelized energy model, 40% of energy consumption was reduced; in addition, the emission of carbon dioxide was 30% degraded [6]; however, for previously constructed buildings, it is costly to replace the glazing. One more research emphasized that glazing type, the orientation of the windows, and the dimension of the glazing should be considered altogether in the design of the glazing to achieve an optimum power performance [7], but once the construction is finished, it will be impossible to change the orientation of the building.

Energy consumption is also related to the window-to-wall ratio (WWR) of the glazing, based on some research, the capacity of the heating and cooling systems required for a building is directly proportional to the WWR ratio [8, 9]. Another study considered the impact of various

✉ Mohammed Lami
b8018683@my.shu.ac.uk

[1] Industry and Innovation Research Institute, Sheffield Hallam University, Sheffield S1 1WB, UK

[2] Department of Oil, Basra Oil Training Institute, Basra, Iraq

[3] Environment and Sustainability Institute, University of Exeter, Exeter, UK

Published online: 20 May 2022

WWR in four directions in Lebanon. The outcome showed a considerable influence of WWR on the annual energy consumption [10]. Similar to building orientation, WWR ratio should be considered at the earlier stage of the construction, else, it will be difficult and costly to modify after construction.

Due to increase in indoor activities of occupants inside premises, studies focused on managing the ventilation systems to ensure air quality inside buildings [11, 12]. Consequently, using of mechanical forced ventilation systems has been rapidly spread recently rather than depending on natural ventilation [13–17]. On the other hand, numerous studies utilised the inlet and outlet air of ventilation systems to inject it inside the cavity of multi pane-glazed windows. The major advantage of this action is to heat up or cool the cavity of windows, consequently, thermal loss through windows can be reduced. For instance, a study introduced a phase change material (PCM) ventilated window, that is, the material that can absorb or release an effective energy when its physical state is changed (usually liquid to solid or vice versa), this feature helps to provide a cooling or heating impact. The study employed a PCM heat-exchanger to pre-heat or pre-cool a double-glazed window. the study concluded that when the window works in heating mode, the temperature of the inlet air is raised by 2 °C along 12 h in the daytime, in addition, when it works in cooling mode, the temperature of the inlet air temperature decreased by 1.4 °C along 7 h in daytime [18].

Other researchers utilise the fresh air or warmed exhausted air to be injected into the double-glazed window (between the panes), this modification helps in reducing the heat transfer coefficient of the window. Lago et al. [19] and Zeyninejad et al. [20] used a solar reflective film with a double-glazed window, the thermal performance of the proposed system has been evaluated. Lago et al. concluded that a spacing of 25 mm between the panes is the best fit to achieve the lowest heat loss during summer. Michaux et al. [21] investigated the thermal performance of a triple-glazed airflow window and then compared it with conventional double-glazed and triple-glazed windows, the result showed a declination in the heating loads of 5% during night and 90% during daytime. Additionally, fifteen windows with different types have been placed in an area by Liu et al. [22], they evaluated the energy performance of the windows and the thermal comfort in the space, the study concluded that using ventilated windows can enhance thermal comfort and reduce the consumption of heating and cooling loads. Another design suggested by Lollini et al. [23], a dynamic glazing system that responds to the outdoor environmental loads, the factors that have an effective influence on the performance of the window like U-value, g-value, spacing airflow thickness, and airflow rate to achieve optimum performance in various weather conditions.

A validated novel design has been introduced by Behrouz Nourozi et al. [24] to minimize the thermal conductivity of the proposed window. The new model has an Argon-filled double-glazed window, in addition, it is sandwiched by another two coated glazing panes. A heat exchanger is employed to provide warmed air to the window. Also, the waste warm air of the building is fed to the heat exchanger, this increases the efficiency of the system. The simulation showed that if the air temperature supplied by the heat exchanger is more than the room temperature, the U-value of the window could be less than 0.65 W/m^2 K. However, the additional components in the new design add more complexity to the structure, which will inflate the installation cost. In addition, when the WWR ratio is high in case of façade buildings that use multiple-glazed windows, the available waste air may not be adequate to heat up the big volume of the cavity between window's panes.

A comparison has been made by Zhang et al. [25] to show the contrast in the performance of a normal triple-glazed and triple-glazed exhaust window, the latter window works in heating/cooling modes and uses the exhaust air from the room to be injected into the window. The study reveals that compared to the conventional window, the exhaust window has the potential to reduce the heating and cooling consumption to 50.1% and 25.3%, respectively. The study assumed that the exhaust air source feeds the window continuously, but if the dimension of the window is big then more air quantity will be needed to maintain a certain level of energy saving.

The previously recalled papers used different sources to inject the air into the gap of the window, some of them preheat the fresh air from the external environment before directing it to the room, while other studies exhaust the air of the room to outdoor environment through the gap to heat the panes during winter or cooling them during summer. It can be concluded that the waste air can be considered as an important resource to maximize the energy saving in a building. Former studies usually assumed that the quantity of the wasted air is unlimited, and the building can continuously feed the proposed ventilation systems to reduce the heat loss through windows. However, in some circumstances the wasted air of a building can be less than expected. For instance, American Society for Heating, Refrigerating, and Air conditioning Engineers ASHRAE recommends that 5 and 4.2 cubic feet of air per minute per person is required to be exchanged with fresh air to ensure a certain level of indoor air quality in large and small buildings, respectively, and a minimum air change per hour of 0.35 [26]. Hence, the available quantity of the wasted air is restricted to number of residents. Consequently, buildings with few occupants may not provide an adequate flow rate for the ventilated windows. Also, the required quantity of wasted air in a building can be determined by the volume of the cavity of the ventilated

multi-glazed windows. However, the volume between glazing panes is a function to the dimension of the window and number of panes. As a result, ventilated windows with a high Window to Wall Ration WWR, especially in façade buildings which can be up to 70% [27–29], the demand of wasted air will be high.

In commercial buildings that equipped with ventilated double-glazed windows, when the available wasted air that used to ventilate the windows is limited due to the earlier mentioned circumstances, thermal performance of the ventilated windows can be effectively declined. Therefore, this paper proposed methods to optimise the utilisation of the wasted air in ventilating of double-glazed windows to maximise the overall energy saving in the building. A multi-scenarios experiment has been conducted on a small-scaled test room. The idea behind the experimental scenarios is sharing the available flow of wasted air to one or multiple windows. Each scenario relies on a different method to share the available wasted air. Sharing of the wasted air is achieved either by distributing the duty of the air-pump among the windows, or by dividing the airflow. The experimental results and heat transfer calculations have been employed to evaluate the thermal performance of the system in different cases. In addition to earlier research on active ventilated windows [19, 24, 30], the present solution optimises the thermal performance of ventilated windows and transforms the window to an energized part in the envelope of buildings instead of the conventional passive windows. As a result, achieving minimal consumption of heating loads and enhance the thermal comfort in the internal environment for occupants.

Methodology and experimental setup

The proposed system

Figure 1 demonstrates the proposed system that will be used to conduct the experiment. A test room has been occupied with a ventilated double-glazed window. A separate small, isolated room is used to generate a warm air (wasted air generation room) with an integrated microcontroller heating system. The generated warm air will be considered as the wasted air during the experiment. The drawn warm air from the wasted air room is compensated from the atmosphere. An air pump is employed to inject the wasted air into the bottom inlet of the window. As a result, the air drifts towards the top outlet of the window and exhausts to the outdoor environment. The inlets and outlets of the wasted air room and the window are occupied with check valves to ensure that the air is flowing in one direction only.

The system operates in three modes: (1) when the air between the panes is kept without circulation, the window acts as a conventional double-glazed window, (2) when the air between the panes is exchanged with the warmed room air at different times or (3) continuously, in this case, the

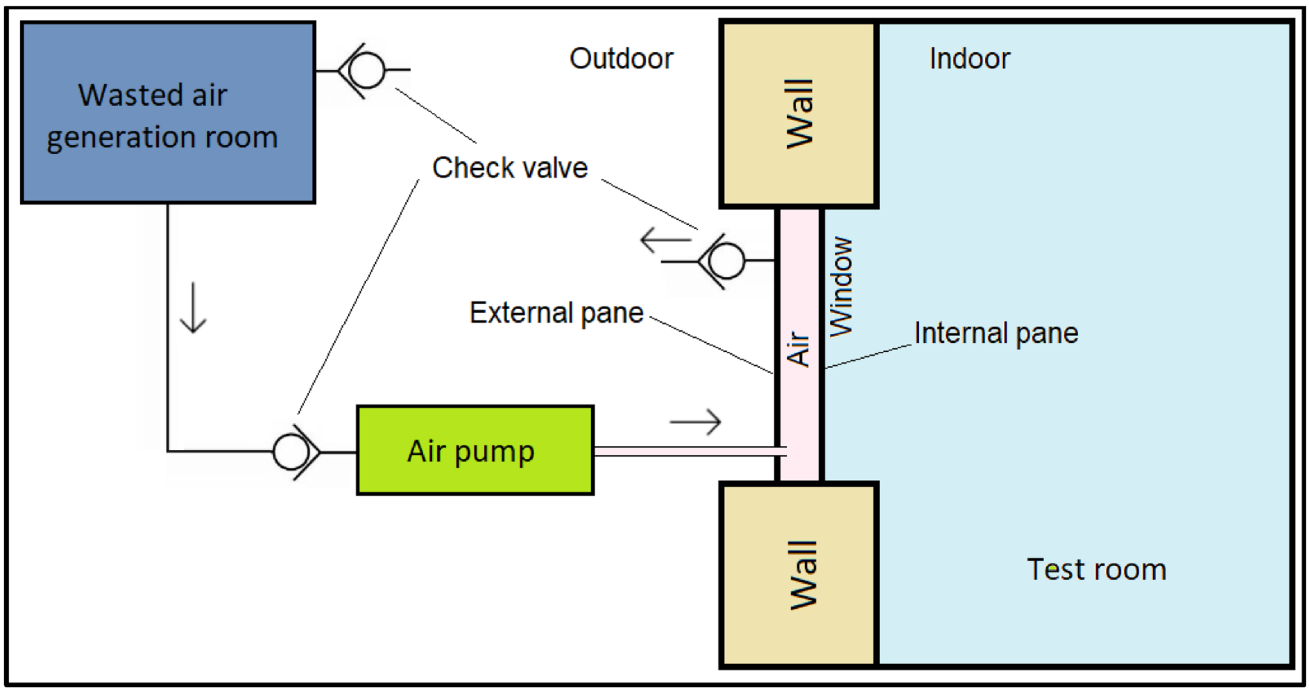

Fig. 1 The integrated double-glazed window

window will be converted to the forced ventilation mode. The three modes are discussed and demonstrated in detail during the implemented experiments in the next sections, in addition to how different cases affect the thermal performance of the window.

Methodology setup

Figure 2 shows the research method setup, which is used to process the work, validate the experimental model, and evaluate the experimental outcome. Two main models have been created in the present study. The first model is the test room model, it is a small-scaled room that will be used to conduct the experiment. The second model is the heat source model, it will be used to demonstrate the thermal response of the heat source used inside the small-scaled room. In other words, the generated heat from the heat source will be fed to the test room. Before conducting the experimental investigations for the case under consideration, a proof-of-concept exercise was carried out. The experimental test room, using the conventional double-glazed window, has been modelled by the commercial Design Builder software. The validation of the established model and the experimental setup will provide a proper reference setup for testing the proposed system and will validate the energy results of the experimental setup when the proposed system is deployed. It is worth mentioning here that the software does not have the options to model the proposed system. However, the following points illustrates the methodology setup shown in Fig. 2 that employed in this paper to achieve the objectives:

1. The initial conditions and other input parameters are obtained from the field by well calibrated sensors. The gathered data includes indoor and outdoor measurements in Fig. 2.
2. For indoor data, test room temperature is essential for heat transfer calculations, also the operation of the heat source and the air-pump are necessary for energy calculations.
3. For outdoor data, the weather data is required to prepare the weather data file to complete the simulation by Design Builder software.
4. The mathematical model of the heat source has been determined using a special calculation process of tungsten filament in the next sections.

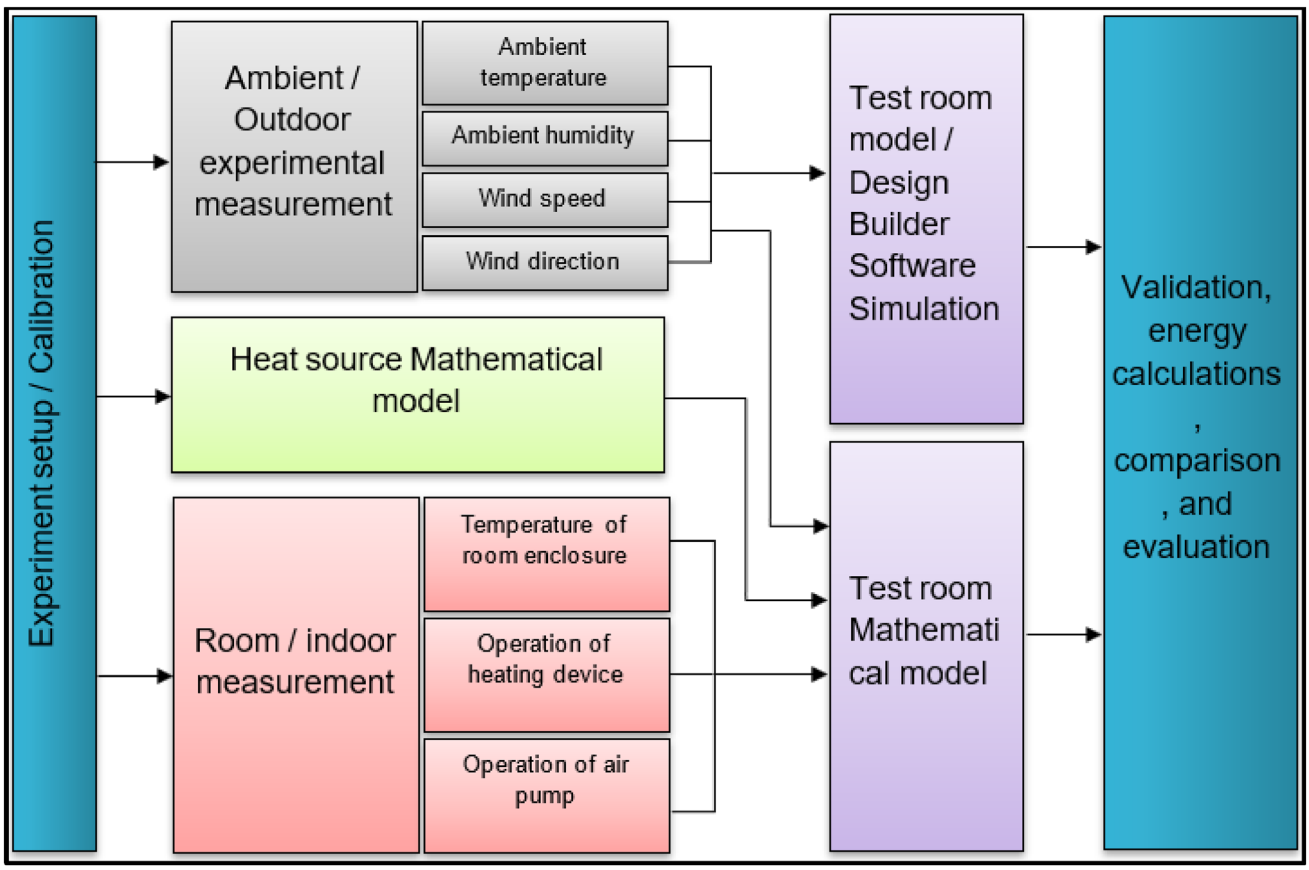

Fig. 2 Research method

5. The standard equations of heat transfer were employed to create the test room model. Heat transfer calculations were used to calculate the overall thermal performance of the window.
6. The mathematical model of the heat source, and the indoor and outdoor measurements provide the input conditions to the mathematical test room model.
7. The thermal performance of both the simulated test room (by Design Builder software) and the mathematical test room model have been compared to validate the system, and to evaluate the overall thermal performance.
8. Finally, the experimental result has been utilised to perform energy calculations and verify the objectives of the study.

Test room

Figure 3-A shows a sketch of the experimental room and the ambient atmosphere. A test room is placed inside a bigger box, the space between the room and the outer box represents the atmosphere. Thus, the experiment can be done in a controlled environment. The temperature of the atmosphere will be controlled by an external cooling system. Figure 3b shows a cross-sectional area for the experimental setup, an external cooling system was used to inject the cooled air into the outer box, the air spreads in the atmosphere space and then is exhausted from small holes to the outside environment keeping it at a specific temperature. The advantage of the outer box is to provide a dark environment for the test room, this helps to investigate the thermal loss through the window without the effect of solar radiation [31].

In Fig. 4, where the experimental setup is shown, the test room, and the outer box have been made from an insulated board. The board consists of a thick layer of polystyrene with a thermal conductivity of 0.046 W/m K, the polystyrene is sandwiched by two thin layers of steel. A 7-inches hose is attached between the front side of the outer box and the external cooling device.

The heat source used in the experiments is a conventional tungsten-based heater. It utilises a tungsten wire with an electrical resistivity of 168 Ω (at room temperature 25 °C) placed inside a pottery base with a mass of (0.53 kg) and heat capacity of (0.85 kJ/kg °C). Table 1 provides details about the test room structure, double-glazed window, the outer box, and the heat source.

Test room model

The experimental test room has a heating source to warm the room. The generated heat should be transferred to the available different parts of the room, which act as thermal loads. For instance, a part of the generated heat warms the internal environment and the pottery, while the residual heat is dissipated by the walls and the glazing of the window. However, the equations introduced in this part are as suggested by Ghosh et al. [32], have been modified to include the heat absorbed by the pottery according to the given heat system as shown below, the subscript "1" is used here for some abbreviations to avoid the duplication in the next sections.

Q_{Tungsten} heat generated by the tungsten wire (W), Q_{pot1} heat stored in the pottery (W), Q_{g} heat transfer through the glazing (W), Q_{room1} heat stored inside the test room (W), M_{room1} mass of the air inside the room, V_{room1} volume of the test room, C_{air} heat capacity of the air = 1.006 kj/kg ℃, T_{in} temperature inside the room in ℃, Q_{w1} heat transfer through inside and outside air convection and conduction through the insulation board wall (W), U_{w1} combined U-value of the test enclosure's wall with inside and ambient air in ($\text{W/m}^2\text{K}$), h_0 outside convection heat transfer coefficient in ($\text{W/m}^2\text{K}$), h_{i} inside convection heat transfer coefficient in ($\text{W/m}^2\text{K}$), L thickness of the insulation board (m), K thermal conductivity of the insulation board in (W/m K), A_{w} area of the insulation board in m^2,

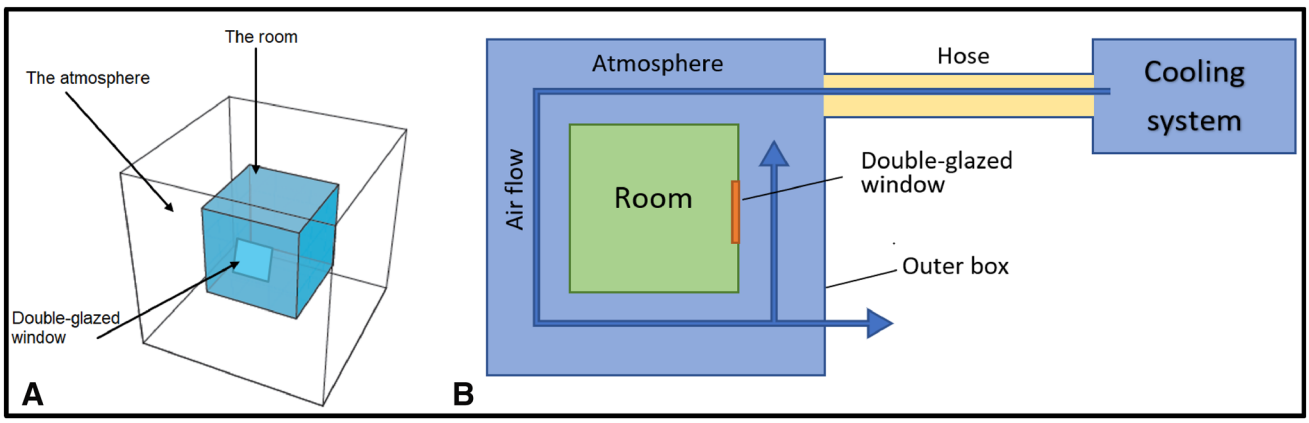

Fig. 3 **a** Test room with the outer box; **b** Cross-section area for the test room with the cooling system

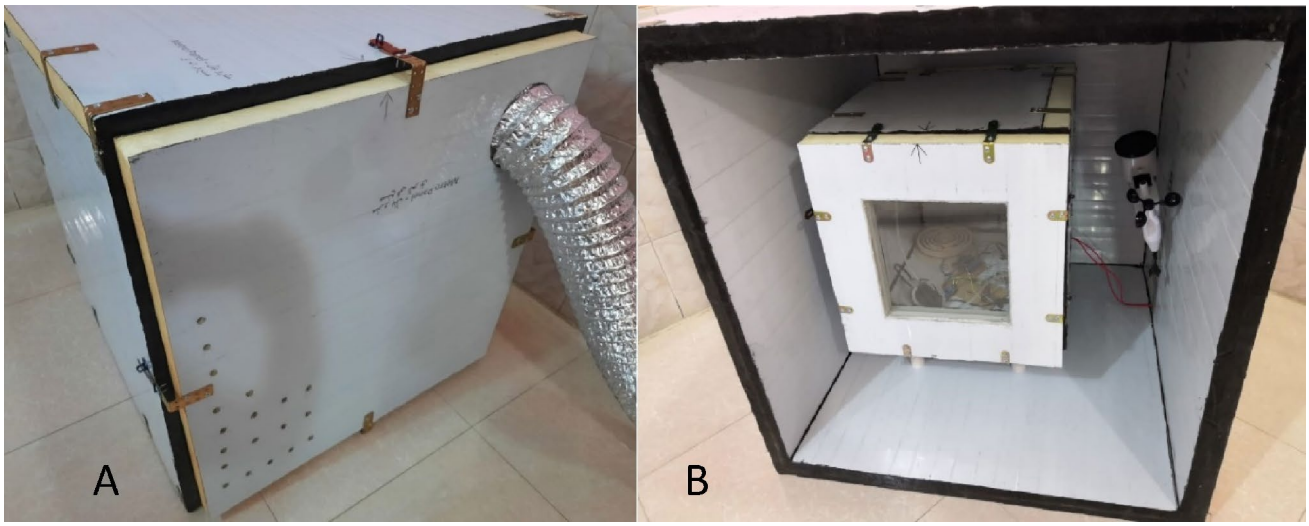

Fig. 4 The experimental setup: **A** The outer box; **B** The test room inside the outer box

Table 1 Specifications of the test room and the outer box

Item	Part	Details
Board	Polystyrene thickness	4.9 cm
	Steel thickness	0.05 cm
Wall dimension of the room		55 × 55 cm^2
Wall dimension of the outer box		100 × 100 cm^2
Double glazed window	Area	30 × 30 cm^2
	WWR	44%
	Glazing type	Clear
	Glazing thickness	0.4 Cm
	Thermal conductivity for the glazing	0.9 W/m K
	Depth of the air layer	2 cm
	Outside reveal depth	0 cm
Room dimension		45 × 45 × 45 cm^3
Outer box dimension		90 × 90 × cm^3
Heat source	AC input voltage	225 V
	Tungsten wire resistance at 25 °C	168 Ω
	Mass of the pottery	0.53 kg
	Heat capacity of the pottery	0.85 kJ/kg °C

T_0 temperature of the atmosphere in ℃, U_g heat transfer coefficient (U-value) of the glazing (W/m^2K), ρ_{air} density of the air = 1.2250 kg/m^3

$$Q_{\text{Tungsten}} = Q_{\text{pot1}} + Q_g + Q_{\text{room1}} + Q_{\text{w1}} \tag{1}$$

Q_{room1} is calculated as following:

$$Q_{\text{room1}} = M_{\text{room1}} C_{\text{air}} \frac{dT_{\text{in}}}{dt} \tag{2}$$

where $M_{\text{room1}} = \rho_{\text{air}} V_{\text{room1}}$.

Q_{w1} can be estimated as following:

$$Q_{\text{w1}} = U_{\text{w1}} A_{\text{w1}} \left(T_{\text{in}} - T_0\right) \tag{3}$$

U_{w1} is determined by:

$$U_{\text{w1}} = \left[\frac{1}{h_o} + \frac{L}{K} + \frac{1}{h_i}\right]^{-1} \tag{4}$$

where $h_0 = 5.7 + 8.8\ V_{\text{wind}}$, V_{wind}: the wind velocity in m/s and $h_i = 7$ (W/m^2 K).

After solving Eq. (1) to find the value of Q_g, then the U-value of the glazing U_g is given in Eq. (5):

$$U_g = \frac{Q_g}{A\left(T_{\text{in}} - T_0\right)} \tag{5}$$

Through cooling period, heat generation of the tungsten wire turns to zero. The pottery starts discharging its heat to the room as it absorbed the effective percentage of heat during heating duration, hence, Eq. (1) can be reformed to match the cooling condition as below:

$$Q_{\text{pot1}} = Q_{\text{g}} + Q_{\text{room1}} + Q_{\text{w1}} \tag{6}$$

Now to determine the net input power to the test room in heating/cooling cases, it is necessary to find the mathematical model of the heat source, represented by the tungsten wire and the pottery. Thus, a new test room will be created to achieve this demand in the next section.

Heat source model

To determine the net input power to the test room in heating/cooling cases, it is necessary to find the mathematical model of the heat source, represented by the tungsten wire and the pottery. A separate experimental model was created. The tungsten-based heat source is placed inside a small box with a dimension of ($0.245 \times 0.175 \times 0.375$ m^3); the same insulated board that used in constructing the test room is utilised for the walls of the box. For easy calculation, the box has been constructed without a window to eliminate the loss through the glazing, also, the purpose of the box is to determine the heat source generation.

Thus, equations of heat transfer model can be adopted to define the heat source model after ignoring the glazing loss, therefore:

Q_{pot2} heat dissipation in the pottery inside the heat source model (W), M_{pot} mass of the pottery = 0.53 kg, C_{pot} heat capacity of the pottery = 0.85 (kj/kg ℃), T_{pot} temperature of the pottery (℃), Q_{room2} heat stored inside the heat source model (W), Q_{w2} heat transfer through inside and outside air convection and conduction through the insulation board wall of heat source model, R electrical resistivity of the tungsten wire at the steady-state temperature, R_0 electrical resistivity of the tungsten wire at the initial temperature, for the executed experiments 25 ℃ and R0 = 168 Ω, T_0 initial temperature of the tungsten wire in kelvin, for the executed experiments 25 ℃ or 298 K, T_{s} steady-state temperature of the tungsten wire in kelvin, T_{s} has been measured experimentally by a K-type thermometer, it was 306 ℃ or 579 K, ν root-mean-square value of the applied ac voltage = 225 V

$$Q_{\text{Tungsten}} = Q_{\text{pot2}} + Q_{\text{room2}} + Q_{\text{w2}} \tag{7}$$

Q_{pot2}: can be calculated as following:

$$Q_{\text{pot2}} = M_{\text{pot}} C_{\text{pot}} \frac{\mathrm{d}T_{\text{pot}}}{\mathrm{d}t} \tag{8}$$

Q_{room2} and Q_{w2} can be estimated using Eq. (2) and (3), respectively, based on the given data of the heat source model.

During cooling period, like the test room model, the input power of the tungsten turns to zero, and the heat stored in the pottery starts transferring to the room as it absorbed the effective percentage of the heat source during heating time, then, Eq. (7) can be reformed to match the cooling condition as below:

$$Q_{\text{pot2}} = Q_{\text{room2}} + Q_{\text{w2}} \tag{9}$$

Before conducting the experimental investigations on the test box, the heat generation characteristics of the source will be estimated and validated. Therefore, the heat source was operated inside the test box, in addition, two calibrated K-type thermocouples were used to measure the temperature inside the room and the temperature of the pottery, as well as a heat sensor outside the box to record the outside temperature. By solving Eq. (7), the heat generation of the source is depicted in Fig. 5. The supplied heat starts increasing once turned on the source and it takes approximately 200 s to approach the steady state. Also, the average steady-state heat generation (from 200 to 600 s) is 117.32 watts.

Agrawal [33] determined the steady state of the heat power for the tungsten wire P as shown in Eqs. (10) and (11):

$$R = R_0 \left(T_{\text{s}}/T_0\right)^x \tag{10}$$

$$P = \frac{v^2}{R_0 \left(T_{\text{s}}/T_0\right)^x} \tag{11}$$

x: the index x is determined to make $R/R_0 = \left(T_{\text{s}}/T_0\right)^x$ based on Eq. (10), the ratio of R/R_0 is obtained from the table of the resistivity of tungsten on [34] in the range of 298–579 K. According to the given data, the best fit of the index x is 1.31.

Solving Eqs. (8) and (9), the steady-state heat generated by the source is 123.46 watts as shown in Fig. 5. The theoretical value of the steady state is quite close to that determined experimentally, 117.32 W, the variation could be because of ignoring the heat absorbed by some objects inside the box such as electrical wires and thermocouple wires. Thus, the experimental model of the heat source can be assumed to be valid for further considerations.

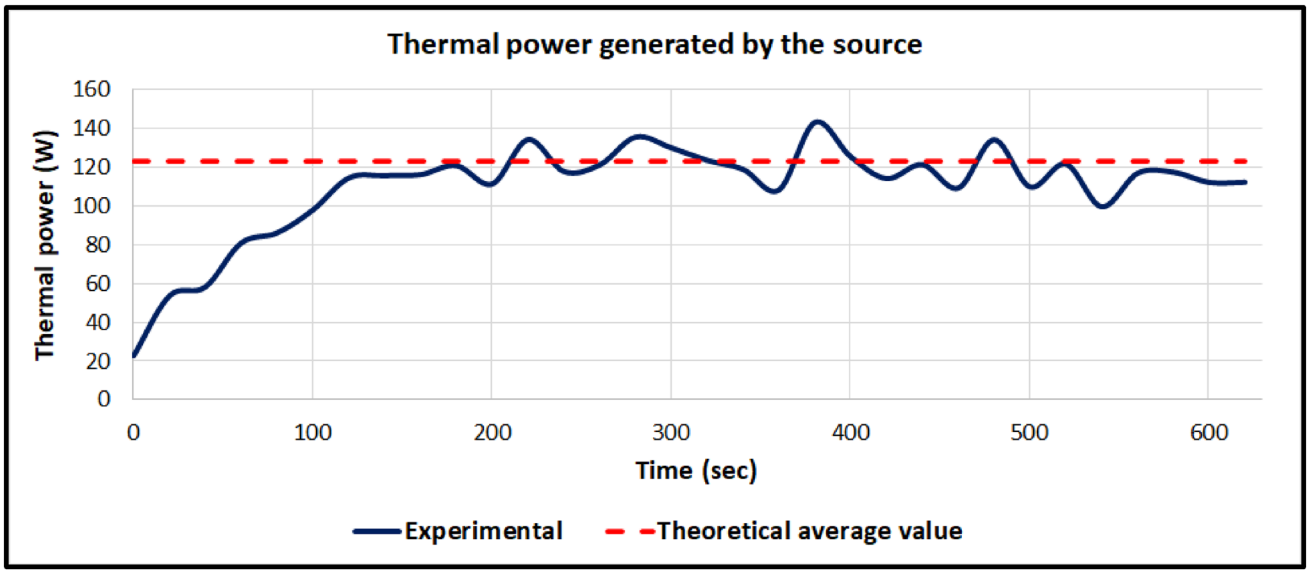

Fig. 5 Heat generation of the tungsten-based heat source

Simulation and validation

A separate experiment has been conducted to validate the test room. The profile of the atmosphere temperature shown in Fig. 6 has been applied on the test room, and the heat source was OFF. Simultaneously, the heat sensor recorded room temperature, while the weather station gathered the atmospheric conditions: temperature, humidity, pressure, and wind speed.

On the other hand, the Design Builder software has been employed to model the test room based on the parameters mentioned in Table 1. Also, the weather data file (required for the simulation) has been prepared to match the experimental conditions; this includes the data measured by the weather station. For the solar and illuminance data, they

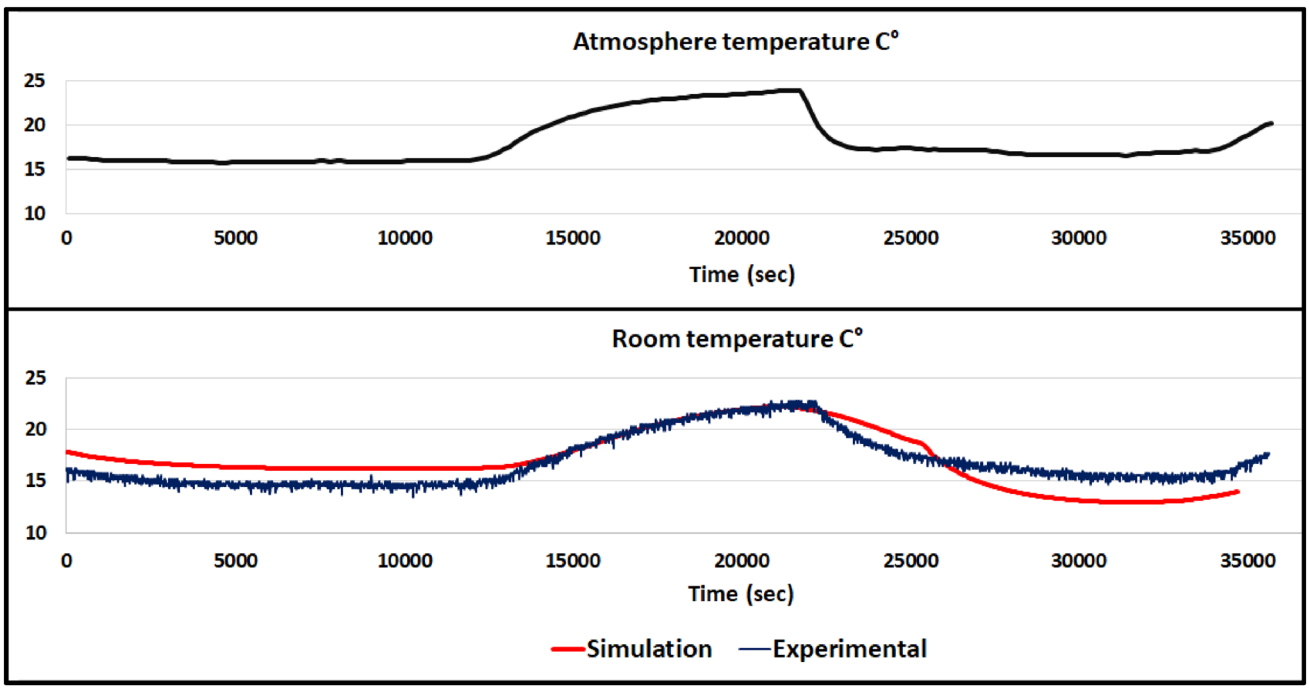

Fig. 6 The validation of the experimental room

were set to zero as the experiment has been executed in a dark space (inside the outer box).

The room temperature has been obtained by the simulation and experimentally as depicted in Fig. 6. The result shows that the simulated and experimental curves are responding according to the variation of the atmosphere condition. Furthermore, the average deviation between the simulated and the experimental room temperature is 0.2 °C. Therefore, it is possible to assume that the experimental test room is a valid reference for further consideration when the proposed system is deployed.

Experiment scenarios

The scenarios shown in Table 2 have been executed on the test room, a logging and a control system were created. It is assumed that the available flow rate of wasted air is only 2000 cc/min in all scenarios. The wasted air will be fed to the proposed ventilated double-glazed window. In each scenario, the main challenge is to consume a minimum possible quantity from the available wasted air, hence, the residual quantity can be exploited for other windows. In this manner, overall energy saving can be maximized. Utilising of wasted air quantity per one ventilated window will be implemented based on the following methods:

i. For the first scenario, the window worked in conventional double-glazed mode as the air pump was OFF. This scenario will be considered as the reference case.
ii. The pump works in a duty cycle of 50% as below:
a. According to the given dimension of the proposed double-glazed window and the maximum available flow of the wasted air (2000 cc/min), the pump should run 54 s to exhaust the air in the cavity of the window and replace it with the wasted warm air. Therefore, in the second scenario, the pump was operated only 54 s and turned off for 54 s during one duty cycle, or an on/off operating frequency of (1/108 Hz).
b. The on/off operating frequency of the pump was increased to (1/20 Hz) and (1/10 Hz) in the third and fourth scenarios, respectively.

The pump works continuously (duty cycle of 100%) with different flow rates. The flow rate of the wasted air was adjusted to 2000 cc/min, 1000 cc/min, 666 cc/min, and 500 cc/min during the fifth to eighth scenarios, respectively.

During each scenario, the test room will pass through two states, heating and cooling. Heating state starts at initial room temperature of 22 °C, the target is to warm up the room to 27 °C; then, the heating device will be turned off. During cooling state, the test room will be left to operate under atmosphere conditions. Cooling interval is the time required for the room temperature to fall to 22 °C.

In the next sections, the results of the eight scenarios will be demonstrated, furthermore, the impact of (1) the duty cycle and on/off operating frequency of the pump and (2) flow rate of the wasted air on thermal performance of the window will be analysed.

Results and discussion

The eight scenarios demonstrated in Table 2 are conducted on the test room inside the outer box. The weather station was fixed in the atmosphere space to record the weather conditions. Also, the test room temperature has been logged by the K-type thermocouple with a time step of 10 s. The temperature of the wasted air was 24.5 °C in all mentioned scenarios.

Figure 7 shows test room temperature when the air pump was off. In this scenario, the window acts as a conventional double-glazed window. This condition will be considered as the reference case. As depicted in the figure, during heating period, it was required to run the heat source 100 s to raise the room temperature from 22 to 27 °C. During the cooling

Table 2 Experimental scenarios

No	Flow rate (cc/min)	Pump duty cycle (%)	Pump on/off frequency (Hz)	Initial room temperature (°C)	Highest room temperature (°C)	Final room temperature (°C)
1	0	0	0	22	27	22
2	2000	50	1/108			
3	2000	50	1/20			
4	2000	50	1/10			
5	2000	100	0			
6	1000	100	0			
7	666	100	0			
8	500	100	0			

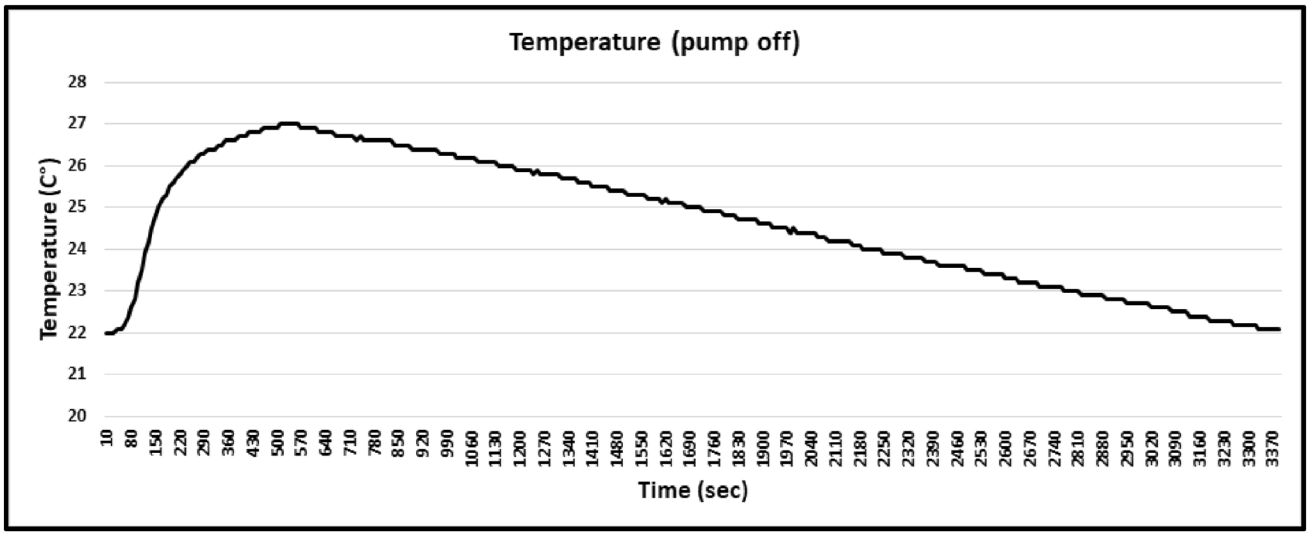

Fig. 7 Test room temperature in scenario 1

period, room temperature declined to 22 °C again after 3390 s.

Figure 8 demonstrates room temperature for scenarios 2, 3, and 4. The window acts as a ventilated double-glazed window. The heat source was required to operate for 100 s during heating period to increase room temperature from 22 to 27 °C. During cooling period, room temperature dropped to 22 °C again after 4690 s, 4830 s, and 4870 s, respectively.

Figure 9 elucidates room temperature for scenarios 5, 6, 7, and 8. The window acts as a ventilated double-glazed window. Room temperature grew from 22 to 27 °C after running the heat source for 100 s during heating period. During cooling period, room temperature declined to 22 °C again after 7230 s, 6420 s, 5120 s, and 4050 s, respectively.

It is noted that temperature of the test room has the same envelope in all scenarios, initial temperature of 22 °C, maximum target temperature of 27 °C, and final target temperature of 22 °C. However, the cooling period varied in different scenarios, as the heat transfer conditions were different in each scenario.

As the heating and cooling durations were not equal in different scenarios, hence, the input heat power is varied in each experiment, because the source needs a time of (200 s) to reach its designated steady-state output. In other words, in the case of heating, the longer the heat source is ON the higher generated power; while in the cooling case, the longer the cooling interval the lower supplied power. In the following steps, the net heat transferred from the source to the test room will be estimated during heating/cooling intervals for all scenarios. Then it will be possible to determine the glazing heat loss and the heat transfer coefficient. However, Table 3 lists heating and cooling intervals of the test room in the implemented experiments. Since the initial and target test room temperature in all scenarios were 22 °C and 27 °C, respectively, heating intervals are slightly different. Therefore, the average heating interval of (594 s) will be considered in the following calculations to avoid redundant results.

During the heating period, referring to Eqs. (1) and (7), the power dissipation in the pottery inside the test room and inside the heat source box are equal $\left(Q_{\text{pot1}} = Q_{\text{pot2}}\right)$, because the heat absorption is the same in both cases, thus, the net heat transferred from the source to the test room is given as follow:

$$\text{Heat supplied to the test room during heating period} = Q_{\text{Tungsten}} - Q_{\text{pot2}} = Q_{\text{room2}} + Q_{\text{w2}} \tag{12}$$

On the other side, referring to Eqs. (6) and (9) that govern cooling state, the power dissipation in the pottery inside the test room and the heat source box are not equal $\left(Q_{\text{pot1}} \neq Q_{\text{pot2}}\right)$, because the temperature difference between the pottery and the room is not the same in both cases. To overcome this obstacle, the difference in heat dissipation of the pottery ΔQ_{pot} can be calculated in terms of the average temperature differences ($T_{\text{pot1av}} - T_{\text{room1av}} = 44 - 24.5 = 19.5$ °C) and ($T_{\text{pot2av}} - T_{\text{room2av}} = 44 - 28.6 = 15.4$ °C), hence, $\Delta T_{1,2} = 19.5 - 15.4 = 4.1$ °C is the temperature difference that causes the deviation between Q_{pot1} and Q_{pot2}, where T_{pot1av} and T_{room1av} are the average temperatures of the pottery and the room in the test room, while T_{pot2av} and T_{room2av} are the average temperatures of the pottery and the room in the heat source box. Thus:

$$\Delta Q_{\text{pot}} = Q_{\text{pot1}} - Q_{\text{pot2}} = M_{\text{pot}} C_{\text{pot}} \frac{\mathrm{d}\left(\Delta T_{1,2}\right)}{\mathrm{d}t} \tag{13}$$

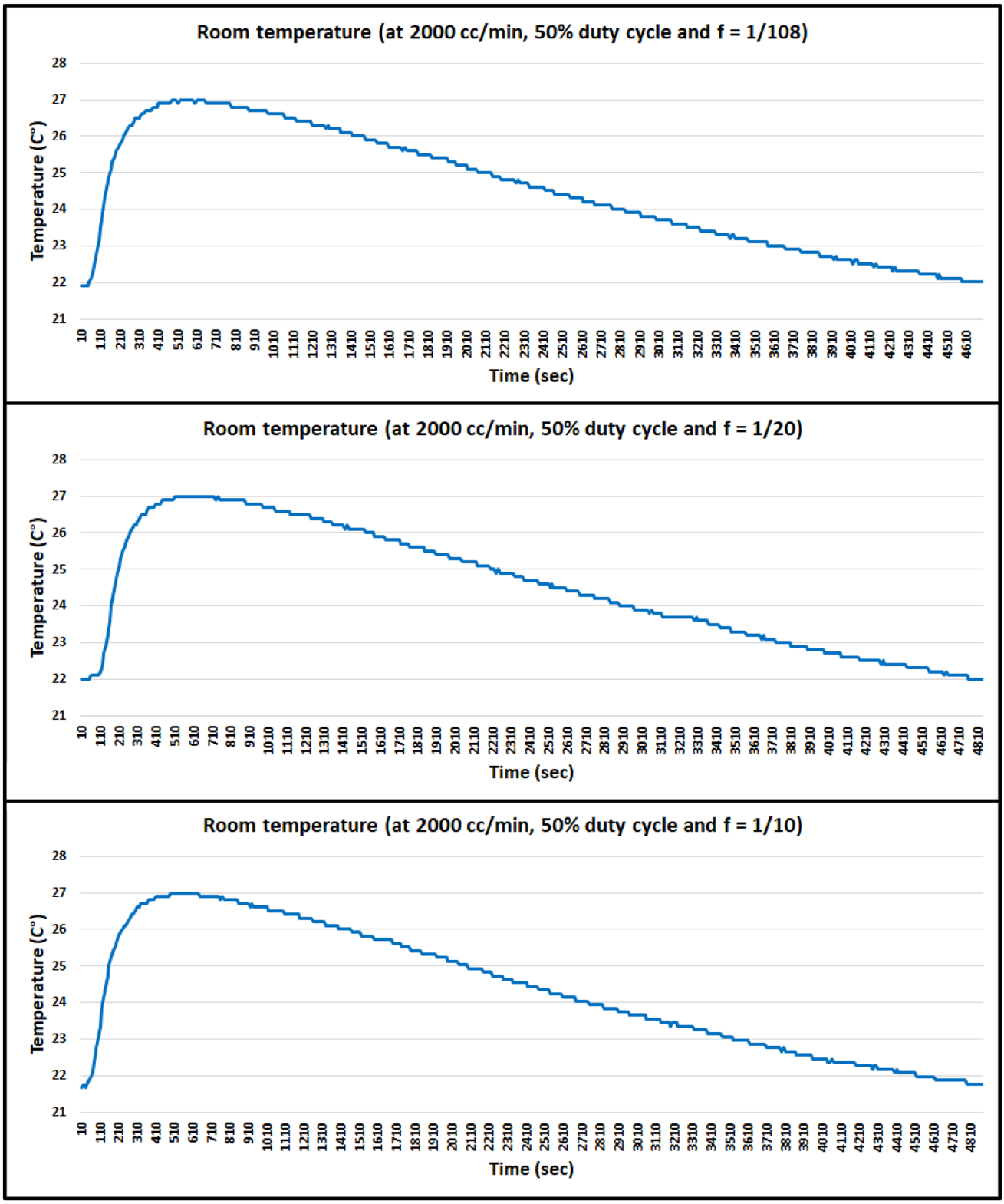

Fig. 8 Test room temperature in scenarios 2, 3, and 4

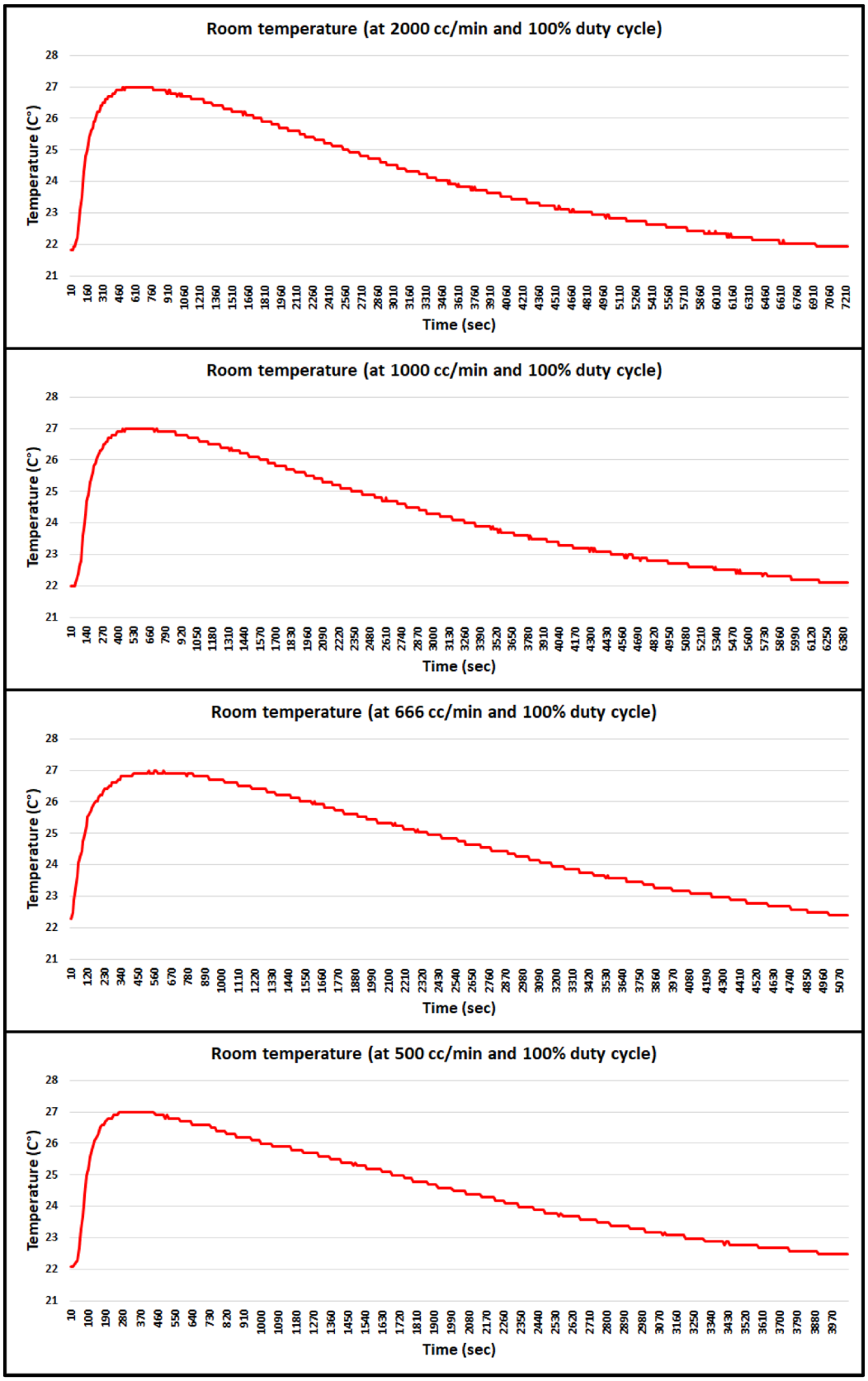

Fig. 9 Test room temperature in scenarios 5, 6, 7, and 8

Hence, the heat supplied to the test room during the cooling period is:

Heat supplied to the test room during cooling period

$$= Q_{pot1} = Q_{room2} + Q_{w2} + \Delta Q_{pot} \quad (14)$$

In all experimental scenarios, the heat source was turned on for 100 s to reach the target temperature, in addition, the longest time required to decrease the test room temperature to 22 °C was in scenario 5, which is 7230 s. Therefore, a separate experiment has been conducted to estimate the average heat supplied to the room during heating and cooling periods in different scenarios. The heat source has been turned on for 100 s inside the box, then the temperature of the room, the pottery and the external environment were taken along 7230 s. The gathered data was used to solve Eq. (12) and (14). Consequently, the heat supplied to the test room during the heating/cooling periods have been estimated as shown in Table 4.

Returning to Eqs. (5) and (6), heat loss in the window Q_g and heat transfer coefficient U_g in the conducted experiments have been estimated. Figures 10, 11, and 12 elucidate the U-value and heat loss of the window in the implemented scenarios. Since the atmosphere temperature is fixed at (17 °C) and only room temperature is varied during the experiments, therefore, glazing heat transfer coefficient and heat loss have same envelope of room temperature. Alternatively, they respond to the temperature

Table 3 Heating/Cooling intervals

Scenario	1	2	3	4	5	6	7	8
Heating period (sec)	560	600	605	610	610	600	610	560
Cooling period (sec)	2830	4090	4225	4260	6620	5820	4510	3490

Table 4 Supplied heat during heating/cooling intervals

Scenario	Average heating period (sec)	Supplied heat (W)	Cooling period (sec)	Average supplied heat (W)
1	594	6	2830	5.1
2			4040	4.68
3			4090	4.43
4			4230	4.32
5			6460	4.36
6			5700	4.25
7			4500	4.51
8			3610	4.86

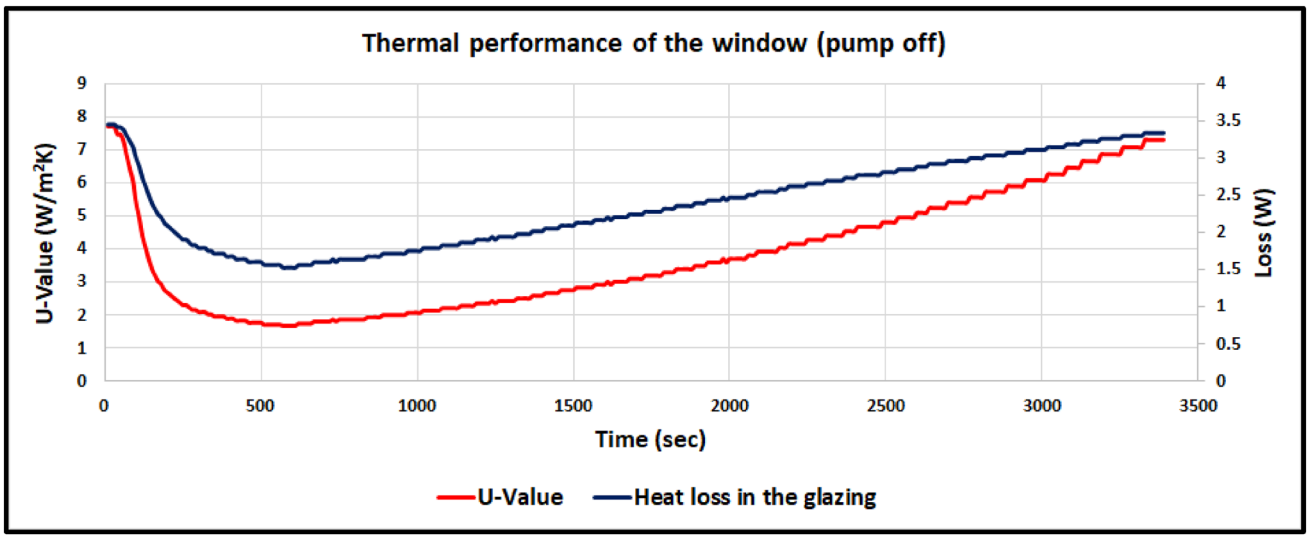

Fig. 10 Glazing U-value and heat loss in scenario 1

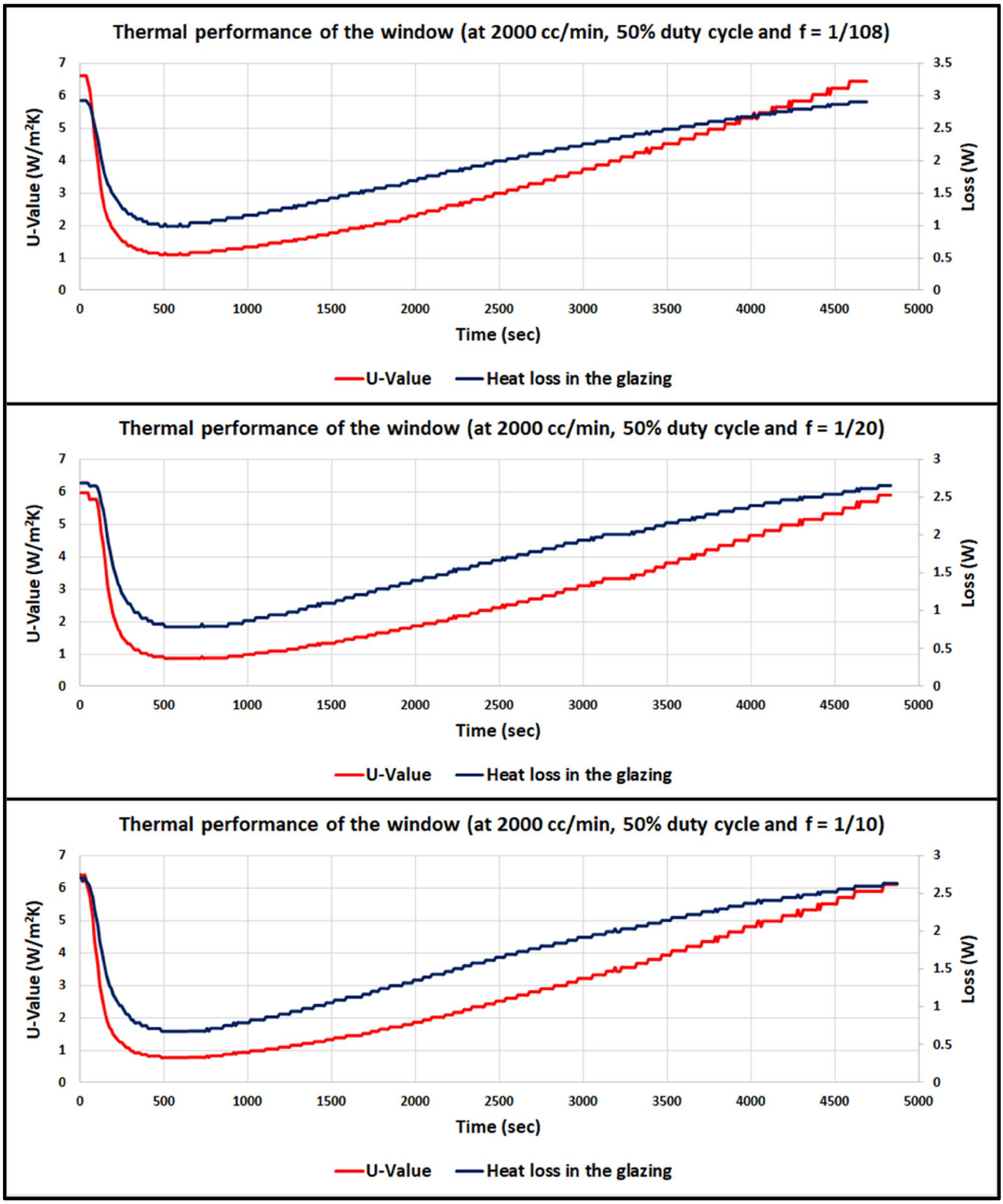

Fig. 11 Glazing U-value and heat loss in scenarios 2, 3, and 4

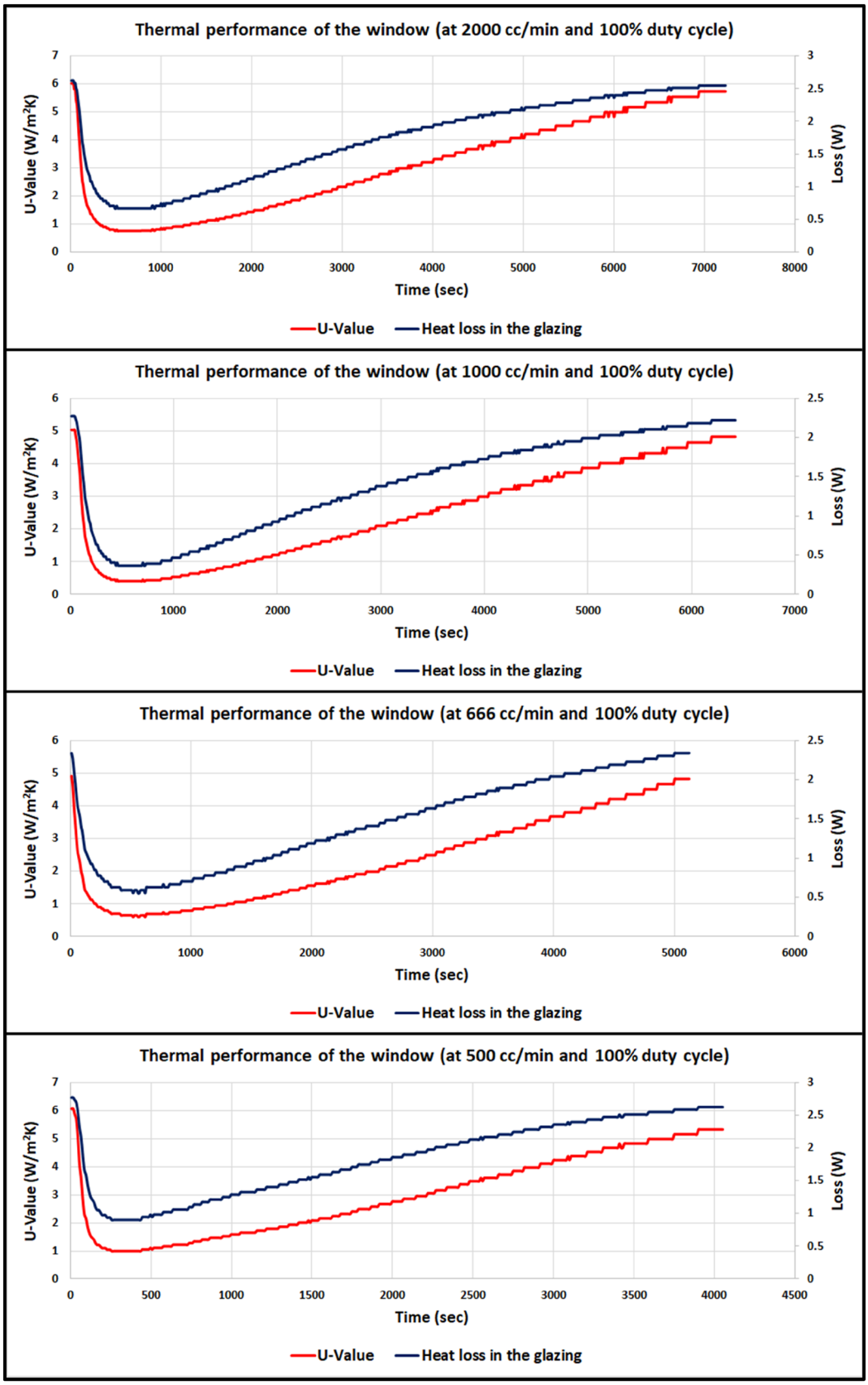

Fig. 12 Glazing U-value and heat loss in scenarios No. 5, 6, 7, and 8

difference between the test room and atmosphere according to Eq. 5. The average values will be considered to investigate the thermal performance of the glazing in different scenarios.

In Fig. 10, thermal performance of the traditional double-glazed window is shown, glazing loss and heat transfer coefficient decreased with the increase in temperature difference between the room and the atmosphere, reflecting an enhancement in the thermal performance during heating period. Oppositely, system performance degraded during the cooling duration while the room temperature is dropping. However, the minimum and maximum recorded values of heat transfer coefficient are 1.7 W/m^2 K and 7.69 W/m^2 K, respectively, and 1.52 W and 3.46 W, respectively, for the glazing loss. For other scenarios 2 to 8 in Figs. 11 and 12, the thermal performance responds to the temperature difference in the same manner. The average values of heat transfer coefficient were 3.24, 2.86, 2.89, 3.06, 2.46, 2.36, and 3 W/m^{2}K, respectively. However, these values reveal a disparate performance in experiment scenarios. In the following paragraphs, the relation between thermal performance and applied conditions in different scenarios will be analysed after completion of energy consumption calculations.

Table 5 illustrates energy calculations in the experiment. Since the operating duration for the heat source are equal in all scenarios (100 s), then the heating device consumed the same energy in different cases. The pump consumption is the product of its power consumption (1.5 W) and the corresponding experiment interval, except in the first case, it equals to zero as the pump was off. Then the total energy consumption is the sum of heating and pump consumption.

Furthermore, Table 6 demonstrates energy saving calculations in the experiment. The experimental intervals of different scenarios are not equal as mentioned earlier. Therefore, to find energy saving for each case, energy consumption in different scenarios should be referred to the first case based on the time (conventional double-glazed window). For instance, the experimental interval in second scenario is 1.38 times that of the first scenario. Therefore, energy consumption in the first scenario is (31,457.5/1.38 = 22,737.9 W sec) with respect to the reference case. In other words, if the test room operates with the condition of scenario 2 for 3390 s (experimental interval of scenario 1), then the consumption would be 22,737.9 W sec. Similarly, energy consumption in other cases have been referred to the first case.

Moreover, energy saving per one window has been estimated for the executed experiments with respect to the

Table 5 Energy calculations

Scenario	Air-pump operation			Experiment duration (sec)	Heating consumption (W sec)	Pump consumption (W sec)	Total consumption (W sec)
	Flow (cc/min)	Duty cycle %	Frequency (Hz)				
1	0	0	0	3390	27,940	0	27,940
2	2000	50	1/108	4690		3517.5	31,457.5
3	2000	50	1/20	4830		3622.5	31,562.5
4	2000	50	1/10	4870		3652.5	31,592.5
5	2000	100	0	7230		10,845	38,785
6	1000	100	0	6420		4815	32,755
7	666	100	0	5120		2560	30,500
8	500	100	0	4050		2025	29,965

Table 6 Energy saving calculations

Scenario	Consumption w.r.t. 1st scenario (W sec)	Energy saving (W sec)	Energy saving per one window (%)	Number of windows can share the available flow	Overall energy saving w.r.t. 1st scenario (%)
1	27,940	–	–	–	–
2	22,737.9	5202.1	18.62	2	37.24
3	22,152.6	5787.4	20.7	2	41.4
4	21,991.5	5948.5	21.3	2	42.6
5	18,185.5	9754.5	34.9	1	34.9
6	17,295.9	10,644.1	38.1	2	76.2
7	20,194.3	7745.7	27.7	3	83.1
8	25,081.8	2858.2	10.2	4	40.8

reference case. The highest saving of 38.1% was achieved with a flow of 1000 cc/min in scenario 6. However, in some scenarios of the experiment, the window utilised the available wasted air partially as shown in table. In this case, it will be assumed that the residual air can be fed to other windows in the building simultaneously to accomplish more energy saving. Consequently, overall energy saving can be illustrated in the following cases:

1. In scenarios 2, 3, and 4, pump duty cycle was 50%, therefore the available flow is adequate to ventilate two windows, hence, overall energy saving will be doubled.
2. In scenario 5, all available flow was used to ventilate only one window, thus, overall energy saving will be the same (34.9%).
3. In scenario 6, the window was ventilated by a flow of 1000 cc/min, hence, two windows can be operated in forced-ventilation mode. Therefore, overall energy saving will be doubled.
4. In scenario 7, a flow of 666 cc/min has been applied on the window, then the 2000 cc/min is adequate to serve three windows. As a result, overall energy saving will be tripled.
5. In scenario 8, the flow was 500 cc/min, therefore it is possible to supply four windows, then overall energy saving will be quadruple.

The experiment demonstrated two kinds of control on the available wasted air to achieve highest possible energy saving. Firstly, in scenario 2, 3, and 4, the pump duty cycle is set to 50%, while the pump turned on/off in different repetitions within its duty. Figure 13 shows the performance of the ventilated window vs on/off intervals control, more details are explained in the following three cases:

1. When the pump works 54 s per one duty cycle, the U-value of the window declined from 3.82 to 3.24 W/m^2 K, achieving an overall energy saving of 37.24% compared to the conventional double-glazed window. During the experiment, it was assumed that turning off the pump for 54 s per one duty cycle could be a long time to allow heat loss to take place through the window. Therefore, a decision has been made to shorten the on/off intervals within one duty cycle in the next steps.
2. After setting on/off intervals of the pump to 10 s per one duty cycle, the system showed a notable improvement in its U-value to be 2.86 W/m^2 K, and an energy saving of 41.4%.
3. With an on/off intervals of 5 s per one duty cycle, the thermal performance was almost saturated, with an energy saving of 42.6% and a U-value of 2.8 W/m^2 K. This was the best obtained performance via controlling the on/off duration as it is not possible to turn the pump on/off within less than 5 s.

Secondly, in scenario 5, 6, 7, and 8, the pump duty cycle was set to 100%, while the window has been fed with different flow rates. Figure 14 demonstrates the performance of the ventilated window vs the flow rate control; more clarifications are elucidated in the following four cases:

1. When the flow rate was set to 2000 cc/min, the U-value of the window declined from 3.82 to 3.07 W/m^2 K,

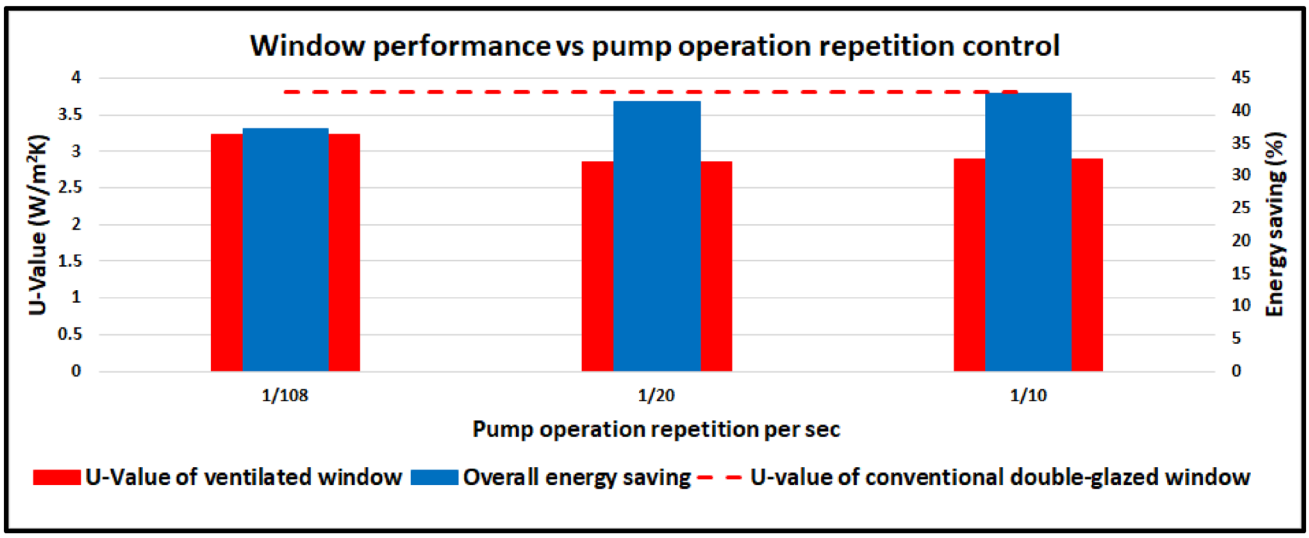

Fig. 13 Ventilated window performance vs on/off intervals control

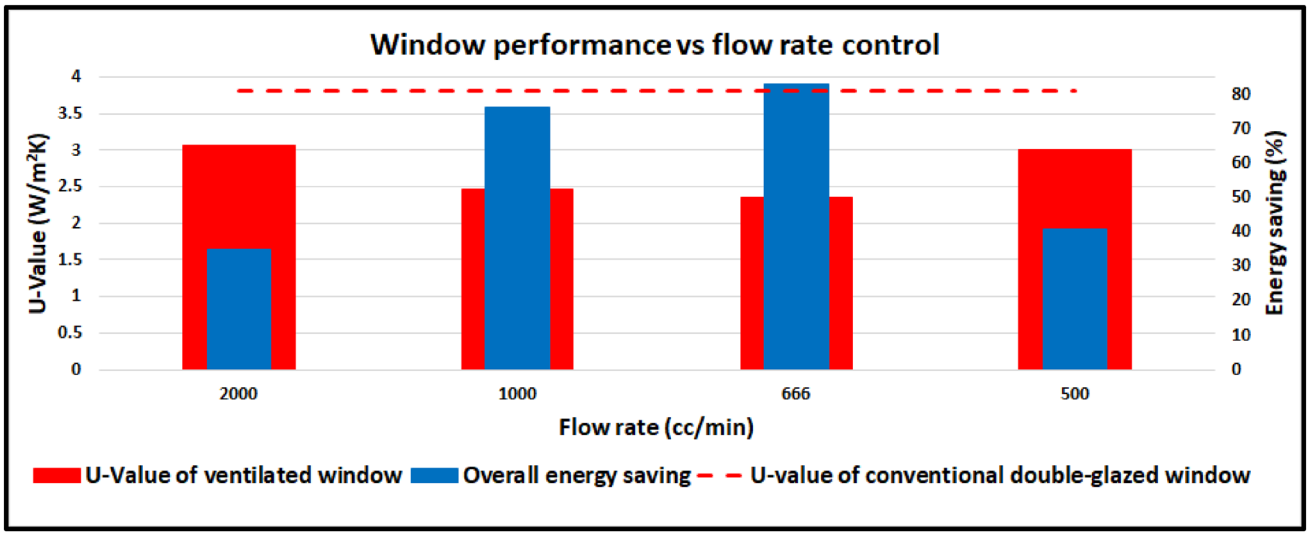

Fig. 14 Ventilated window performance vs flow rate control

achieving an overall energy saving of 34.9% compared to the conventional double-glazed window.

2. With a flow rate of 1000 cc/min, the U-value of the window fell to 2.46 W/m^2 K, and an energy saving of 38.1% has been accomplished. However, as the available waste air can drive two windows with same thermal performance, an overall energy saving of 76.2% can be achieved.
3. The system showed a slight enhancement in the U-value of the window and an overall energy saving of 83.1% with a flow rate of 666 cc/min. It is worth noting that the available flow can drive three windows simultaneously.
4. Heat transfer coefficient has been declined when the flow was adjusted to 500 cc/min, achieving an overall energy saving of 40.8%.

To sum up the method of the conducted scenarios, when the wasted air is distributed by choosing the optimum on/off interval for the pump (in scenarios 2 to 4), the first interval should be opted that completely fills the cavity of the window every time the pump is on. The attempts should be repeated using shorter periods, until the minimum possible interval for the pump. The longer on/off interval allows more heat to be lost through the window while the pump is off. However, the optimum interval is the one that realise a highest energy saving. On the other side, when the wasted air is shared by dividing the flow (in scenarios 5 to 8), multiple attempts should be conducted on single window, two, three windows, and so on, then the optimum number of windows can be considered when a highest energy saving is achieved.

Comparing to the first scenario, the major change in scenarios 2 to 8 that led to enhance the thermal performance is increasing the velocity and the temperature of the air inside the cavity by the forced ventilation. This modification affects the rate of convective heat transfer in the gap of the window [24]. The result shows that cooling span of the test room is related to (1) pump on/off interval, (2) the flow rate of the wasted air, and (3) number of windows can share the available wasted air. For instance, the best performance of the system took place when three windows shared the assumed available flow rate (2000 cc/min) simultaneously. Under this condition, the thermal conductance of the window is decreased, as a result, the room becomes able to maintain the desired temperature range for a longer period.

The proposed system showed that the heat transfer coefficient of the window is adapted to the management of utilising the available wasted air, this is conditioned to the constancy of other factors related to the thermal performance. However, the present paper studied only the effect of heat transfer due to conduction and convection. For instance, solar radiation has an effective impact on the thermal performance of the window, the increase in outdoor temperature can reduce the temperature difference across the window, hence the overall glazing heat loss can be dropped. Similarly, deploying the proposed method in hot regions could be a feasible choice to minimize the cooling loads of buildings. In this case, the cooled air will be injected into the double-glazed window. However, heat storage due to solar irradiance reduces window ventilation efficiency because it inflates the cooling loads [35–37].

Various factors can impact the proposed methods of wasted air management. For instance, number of occupants determines air change per hour in a building, therefore, the more residents the more expected available wasted air. The higher flow rate of the air mitigates heat conduction and convection through the window, as a result energy saving

can be inflated. In addition, high difference between the designated indoor comfort temperature and outdoor temperature increases the heat current through windows, consequently, higher flow rate of the wasted air is required to sustain a same level of heat transfer. In modern design of buildings, it is necessary to opt windows with high WWR ratio to maintain a certain level of visual comfort towards external views and to provide a luminous indoor environment for occupants. However, increasing the dimension of windows add a challenge to provide a higher flow rate for window ventilation. Therefore, such practical cases elucidate the importance of managing the use of the wasted air in buildings.

Circulating of the warmed air through the cavity of windows is also used by other studies to increase the efficiency of double-glazed windows, for instance, Nourozi et al. [24] concluded and stated explicitly that increasing the velocity of the circulated air leads to a declination in the U-value of the window. The authors designed a complex structure and used Argon gas to reduce the thermal conductivity of the window. In addition, they used a separate heat-exchanger to warm up the air before injecting it to the window. As a result, it was possible to reduce the U-value to 0.2 W/m2K which reflects a very efficient performance, this is logical as they paid more. However, this complexity in their system is worthy to be added in the extremely cold regions. While what this study tried to demonstrate is, in the average climate regions where very efficient windows are not needed, the experiment result showed with aid of the mathematical model of heat transfer system that the proposed wasted air management system can achieve an energy saving up to 83.1% in heating consumption. For an already constructed building, the proposed method could be much easier and a cheaper option to be applied than exchanging the windows with triple-glazed windows or other modern types.

As mentioned earlier that higher velocity and temperature of the wasted air leads to a better thermal performance of the ventilated window [24], however, raising of air velocity requires more flow rate, which means more quantity of air. The available volume of the wasted air in a building is determined by the designated air-change-per-hour of the forced ventilation system [26].

In the present study, the test room operates in a dark environment to ignore the effect of solar radiation on the thermal performance of the window. However, in practical applications where the ventilated windows are influenced by the sun, heat storage inside buildings will be exacerbated due to the solar irradiance effect. Consequently, the overall thermal performance of the proposed ventilated window will be higher.

Wasted air management strategies proposed by the present study depends on sharing the available wasted air to ventilate maximum possible number of windows to achieve highest possible energy saving. Therefore, the main challenge that may face the proposed system is the availability of the wasted air regardless the method of sharing the air.

Considering the best performance in scenario 7, an annual energy saving of 56.5 kWh can be achieved in the heating load of the three small-scaled test rooms. In the same manner, if a real-dimension room such as 6×5 m^2 and a height of 3 m is equipped with the proposed ventilated window, an annual consumption of 40.6 MWh will be saved, furthermore, for a building of 30 rooms, the annual energy saving will be 1.22 GWh.

Conclusion

This paper aimed to optimise the utilisation of the wasted air in ventilation of double-glazed windows to achieve highest possible energy saving in heating loads. Optimisation process has been deployed using two methods, both methods rely on sharing the wasted air to multiple windows. The first method is a time-based division of air pump operation, an air pump ventilates multiple windows, one window at a time repetitively. The second method shares the available wasted air to multiple windows simultaneously. The experimental results and heat transfer calculations have been employed to evaluate the thermal performance of the system. The main findings are:

1. The overall energy saving of heating loads in a building can be maximized by distributing the wasted air to multiple ventilated double-glazed windows.
2. The first ventilation method showed a best energy saving of 50%, with a duty cycle of 50%, i.e. the wasted air was supplied to two windows, and on/off operation every 10 s. An energy saving of 42.6% has been realized compared to the traditional double-glazed windows, and the heat transfer coefficient was declined from 3.82 to 2.8 W/m^2 K.
3. The second method showed an optimum thermal performance when the available flow rate of the wasted air was fed to three double-glazed windows simultaneously. An energy saving of 83.1% was achieved compared to the traditional double-glazed windows, and the heat transfer coefficient was dropped from 3.82 to 2.36 W/m^2 K.

Therefore, this study recommends considering the proposed strategies in the earlier design stages of commercial buildings in cold regions. In addition, due to the simple structure of the proposed system, it can be applied to the double-glazed windows in old buildings easily with low cost. However, for a building, the designated air change per hour, flow rate and temperature of the wasted air, number of occupants, window to wall ratio, indoor comfort temperature and

outdoor conditions impact the proposed ventilation methods of double-glazed windows in the practical applications. Overall, applying the proposed wasted air management methods can effectively enhance the thermal performance of the ventilated windows and maximize energy saving of heating loads in cold environments.

Declarations

Conflict of interest The authors have no competing interests to declare that are relevant to the content of this article. The authors declare that they have no conflict of interest.

References

1. Li, H.W.S.G.: Summarization of present building energy consumption and corresponding strategies in China. Environ. Sci. Manag. **33**(2), 6–9 (2008)
2. International Energy Agency, Statistics and Data. (2018). https://www.iea.org/
3. Zemitis, J., Borodinecs, A.: Energy saving potential of ventilation systems with exhaust air heat recovery. IOP Conf. Ser. Mater. Sci. Eng. (2019). https://doi.org/10.1088/1757-899X/660/1/012019
4. Lu, N., Taylor, T., Jiang, W., Correia, J., Leung, L.R., Wong, P.C.: The temperature sensitivity of the residential load and commercial building load. In: 2009 IEEE Power and Energy Society General Meeting, PES '09 (2009). https://doi.org/10.1109/PES.2009.5275654
5. Jiang, Z. and Rahimi-Eichi, H.: Design, modeling and simulation of a green building energy system. In: 2009 IEEE Power and Energy Society General Meeting, PES '09, pp. 1–7 (2009). https://doi.org/10.1109/PES.2009.5275755.
6. Eljojo, A.: Effect of windows size, position and orientation on the amount of energy needed for winter heating and summer cooling. J. Eng. Res. Technol. (2017). https://doi.org/10.13140/RG.2.2.32424.47361
7. Muhaisen, A.S., Dabboor, H.R.: Studying the impact of orientation, size, and glass material of windows on heating and cooling energy demand of the gaza strip buildings. J. Archit. Plan. **27**(1), 1–15 (2015)
8. Youssef, A.M.A., Zhai, Z.J., Reffat, R.M.: Design of optimal building envelopes with integrated photovoltaics. Build. Simul. **8**(3), 353–366 (2015). https://doi.org/10.1007/s12273-015-0214-y
9. Cannavale, A., Ayr, U., Martellotta, F.: Energetic and visual comfort implications of using perovskite-based building-integrated photovoltaic glazings. Energy Procedia **126**, 636–643 (2017). https://doi.org/10.1016/j.egypro.2017.08.256
10. Saridar, S., Elkadi, H.: The impact of applying recent façade technology on daylighting performance in buildings in eastern Mediterranean. Build. Environ. **37**(11), 1205–1212 (2002). https://doi.org/10.1016/S0360-1323(01)00095-6
11. Dockery, D.W.: Health effects of particulate air pollution. Ann. Epidemiol. **19**(4), 257–263 (2009). https://doi.org/10.1016/j.annepidem.2009.01.018
12. Yamaguchi, N., Ichijo, T., Sakotani, A., Baba, T., Nasu, M.: Global dispersion of bacterial cells on Asian dust. Sci. Rep. (2012). https://doi.org/10.1038/srep00525
13. Wieser, A.A., Scherz, M., Passer, A., Kreiner, H.: Challenges of a healthy built environment: air pollution in construction industry. Sustainability (Switzerland) (2021). https://doi.org/10.3390/su131810469
14. Cuce, E., Harjunowibowo, D., Cuce, P.M.: Renewable and sustainable energy saving strategies for greenhouse systems: a comprehensive review. Renew. Sustain. Energy Rev. **64**, 34–59 (2016). https://doi.org/10.1016/j.rser.2016.05.077
15. Elhadary, M.I., Alzahrani, A.M.Y., Aly, R.M.H., Elboshy, B.: A comparative study for forced ventilation systems in industrial buildings to improve the workers' thermal comfort. Sustainability (Switzerland) (2021). https://doi.org/10.3390/su131810267
16. Amaral, R.E.C., et al.: Waste management and operational energy for sustainable buildings: a review. Sustainability (Switzerland) (2020). https://doi.org/10.3390/su12135337
17. Park, S., Park, H., Seo, J.: Analysis on the exhaust air recirculation of the ventilation system in multi-story building. Appl. Sci. (Switzerland) (2021). https://doi.org/10.3390/app11104441
18. Hu, Y., Heiselberg, P.K., Guo, R.: Ventilation cooling/heating performance of a PCM enhanced ventilated window-an experimental study. Energy Build. **214**, 109903 (2020). https://doi.org/10.1016/j.enbuild.2020.109903
19. Lago, T.G.S., Ismail, K.A.R., Lino, F.A.M.: Ventilated double glass window with reflective film: modeling and assessment of performance. Sol. Energy **185**, 72–88 (2019). https://doi.org/10.1016/j.solener.2019.04.047
20. Movassag, S.Z., Zamzamian, K.: Numerical investigation on the thermal performance of double glazing air flow window with integrated blinds. Renew. Energy **148**, 852–863 (2020). https://doi.org/10.1016/j.renene.2019.10.170
21. Michaux, G., Greffet, R., Salagnac, P., Ridoret, J.B.: Modelling of an airflow window and numerical investigation of its thermal performances by comparison to conventional double and triple-glazed windows. Appl. Energy **242**, 27–45 (2019). https://doi.org/10.1016/j.apenergy.2019.03.029
22. Liu, M., Heiselberg, P.K., Larsen, O.K., Mortensen, L., Rose, J.: Investigation of different configurations of a ventilated window to optimize both energy efficiency and thermal comfort. Energy Procedia **132**, 478–483 (2017). https://doi.org/10.1016/j.egypro.2017.09.660
23. Lollini, R., Danza, L., Meroni, I.: Energy efficiency of a dynamic glazing system. Sol. Energy **84**(4), 526–537 (2010). https://doi.org/10.1016/j.solener.2009.12.006
24. Nourozi, B., Ploskić, A., Chen, Y., Chiu, J.N.-W., Wang, Q.: Heat transfer model for energy-active windows–an evaluation of efficient reuse of waste heat in buildings. Renew. Energy **162**, 2318–2329 (2020). https://doi.org/10.1016/j.renene.2020.10.043
25. Zhang, C., Gang, W., Wang, J., Xu, X., Du, Q.: Numerical and experimental study on the thermal performance improvement of a triple glazed window by utilizing low-grade exhaust air. Energy **167**, 1132–1143 (2019). https://doi.org/10.1016/j.energy.2018.11.076

26. ASHRAE, Standard 62.1, Ventilation for Acceptable Indoor Air Quality; American Society of Heating, Refrigerating and Air conditioning Engineers. Atlanta, GA, USA (2004)
27. Sayadi, S., Hayati, A., Salmanzadeh, M.: Optimization of window-to-wall ratio for buildings located in different climates: an IDA-indoor climate and energy simulation study. Energies (2021). https://doi.org/10.3390/en14071974
28. Shaeri, J., Habibi, A., Yaghoubi, M., Chokhachian, A.: The optimum window-to-wall ratio in office buildings for hot-humid, hot-dry, and cold climates in Iran. Environments MDPI (2019). https://doi.org/10.3390/environments6040045
29. Goia, F.: Search for the optimal window-to-wall ratio in office buildings in different European climates and the implications on total energy saving potential. Sol. Energy **132**, 467–492 (2016). https://doi.org/10.1016/j.solener.2016.03.031
30. Casini, M.: Active dynamic windows for buildings: a review. Renew. Energy **119**, 923–934 (2018). https://doi.org/10.1016/j.renene.2017.12.049
31. Fung, T.Y.Y., Yang, H.: Study on thermal performance of semi-transparent building-integrated photovoltaic glazings. Energy Build. **40**(3), 341–350 (2008). https://doi.org/10.1016/j.enbuild.2007.03.002
32. Ghosh, A., Norton, B., Duffy, A.: Measured overall heat transfer coefficient of a suspended particle device switchable glazing. Appl. Energy **159**, 362–369 (2015). https://doi.org/10.1016/j.apenergy.2015.09.019
33. Agrawal, D.C.: Heating-times of tungsten filament incandescent lamps. Science **15**, 86–97 (2018)
34. Jones, H.A.: The Characteristics of Tungsten Filaments as Functions of Temperature. Pergamon Press Ltd, London (1960). https://doi.org/10.1016/b978-1-4831-9910-8.50023-9
35. Shrestha, A., Shimizu, T.: Evaluation of the suppressive effects on solar radiation for a building façade covered with green layers in the Kathmandu valley. Environ. Chall. **5**, 100246 (2021). https://doi.org/10.1016/j.envc.2021.100246
36. Mas, Ł.Y.D., Sitek, M., Fross, K.: The impact of solar radiation on the quality of buildings: Research methods. In: Lecture Notes in Computer Science (including subseries Lecture Notes in Artificial Intelligence and Lecture Notes in Bioinformatics), vol. 9178, pp. 322–331 (2015). https://doi.org/10.1007/978-3-319-20687-5_31
37. Shohan, A.A.A., Al-Khatri, H., Bindajam, A.A., Gadi, M.B.: Solar gain influence on the thermal and energy performance of existing mosque buildings in the hot-arid climate of Riyadh city. Sustainability (Switzerland) (2021). https://doi.org/10.3390/su13063332